

Supplemental Figures and Table for:

STING Activation Reprograms the Microenvironment to Sensitize NF1-related Malignant Peripheral Nerve Sheath Tumors for Immunotherapy

Bandarigoda N. Somatilaka¹, Laasya Madana¹, Ali Sadek¹, Zhiguo Chen¹, Sanjay Chandrasekaran^{2,3}, Renee M. McKay¹, and Lu Q. Le^{1,2,4,5,6,7}

¹Department of Dermatology, ²Simmons Comprehensive Cancer Center, ³Department of Internal Medicine, Division of Hematology/Oncology, ⁴UTSW Comprehensive Neurofibromatosis Clinic, ⁵Hamon Center for Regenerative Science and Medicine, ⁶O'Donnell Brain Institute, University of Texas Southwestern Medical Center at Dallas, Dallas, Texas, 75390-9069, USA, ⁷Department of Dermatology, University of Virginia School of Medicine, Charlottesville, VA, 22903, USA

Author for correspondence:

Lu Q. Le, M.D., Ph.D.
Professor and Chair
Department of Dermatology
University of Virginia School of Medicine
Phone: (434) 982-5974
Fax: (434) 244-4504
E-mail: bkn6qd@uvahealth.org

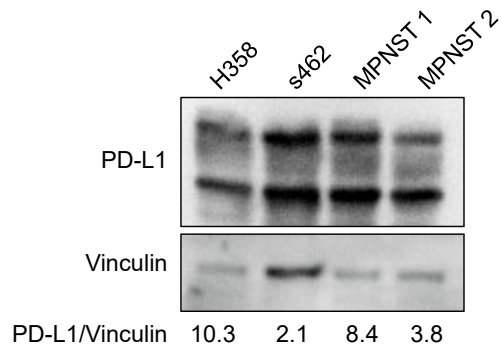
Short title: Reprogramming MPNST for immune checkpoint blockade

Conflicts of interest: The authors have declared that they have no competing interests.

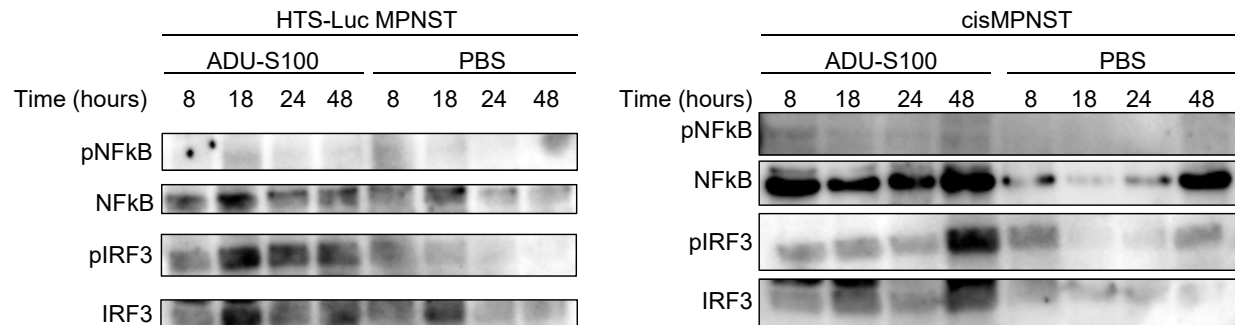
Keywords

Neurofibromatosis Type 1, NF1, neurofibroma, plexiform neurofibroma, malignant peripheral nerve sheath tumor, MPNST, STING, immune checkpoint blockade, ICB, ADU-S100

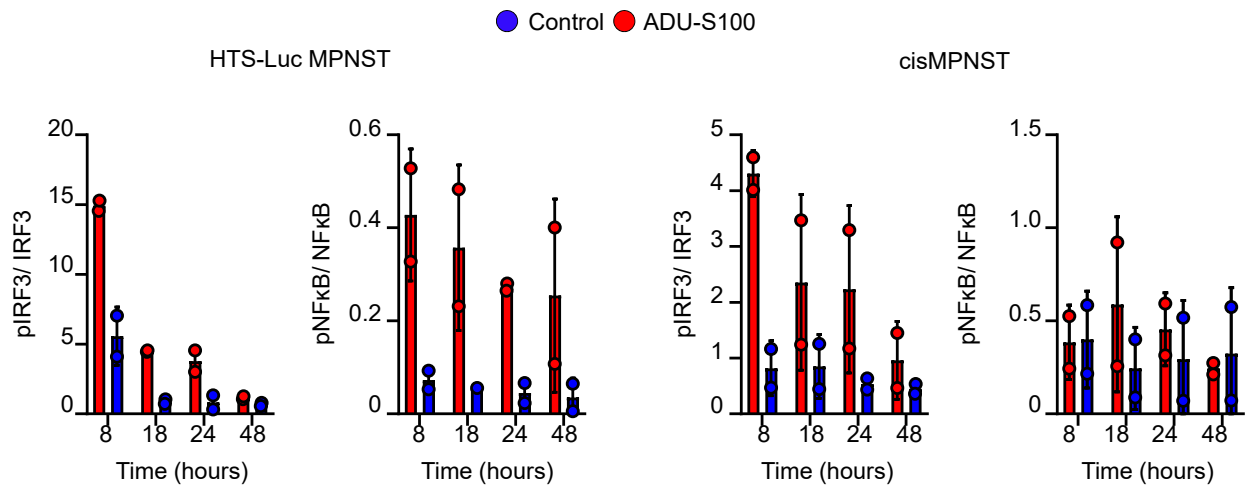
A



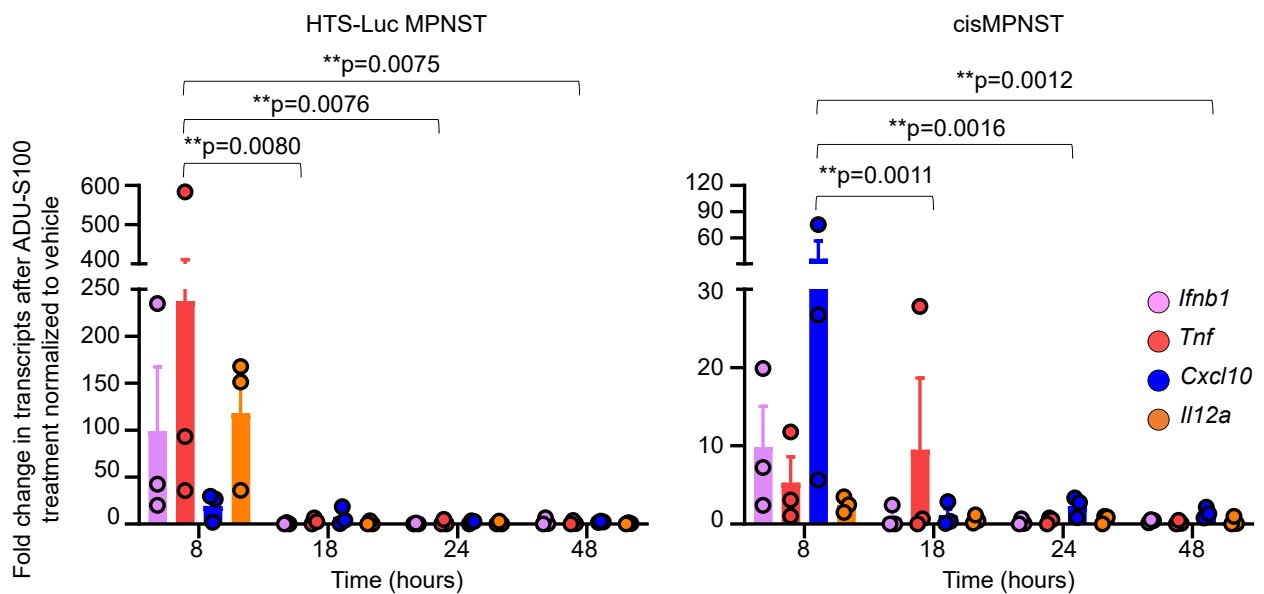
B



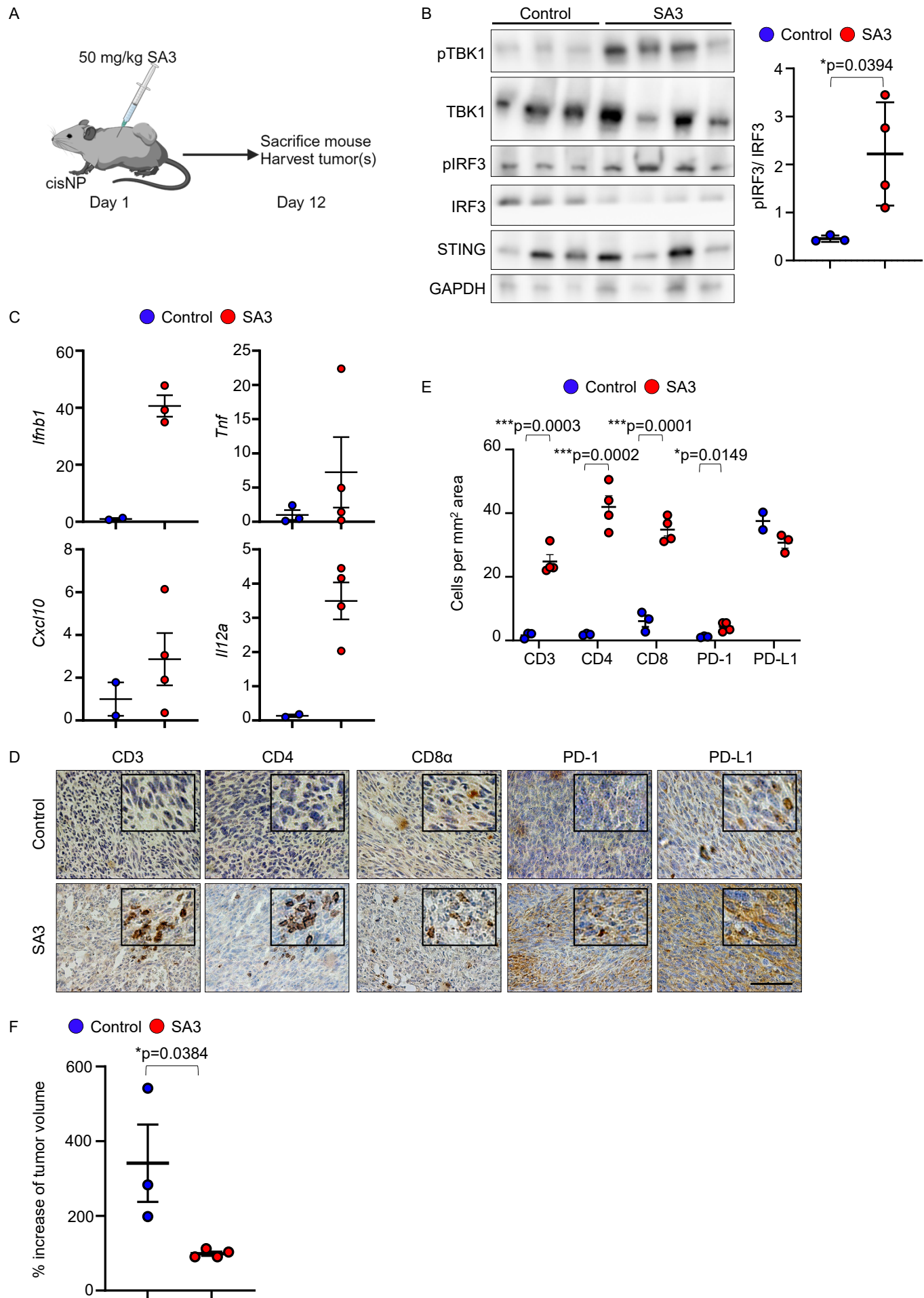
C



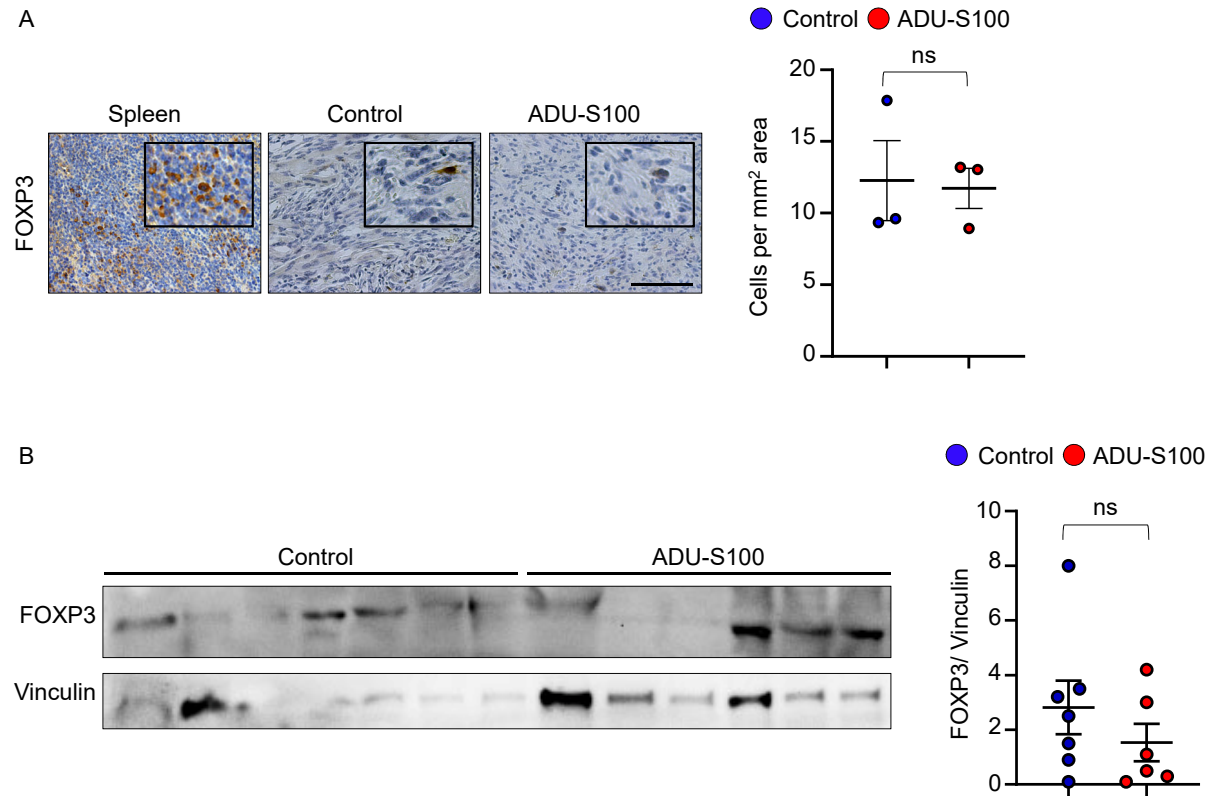
D



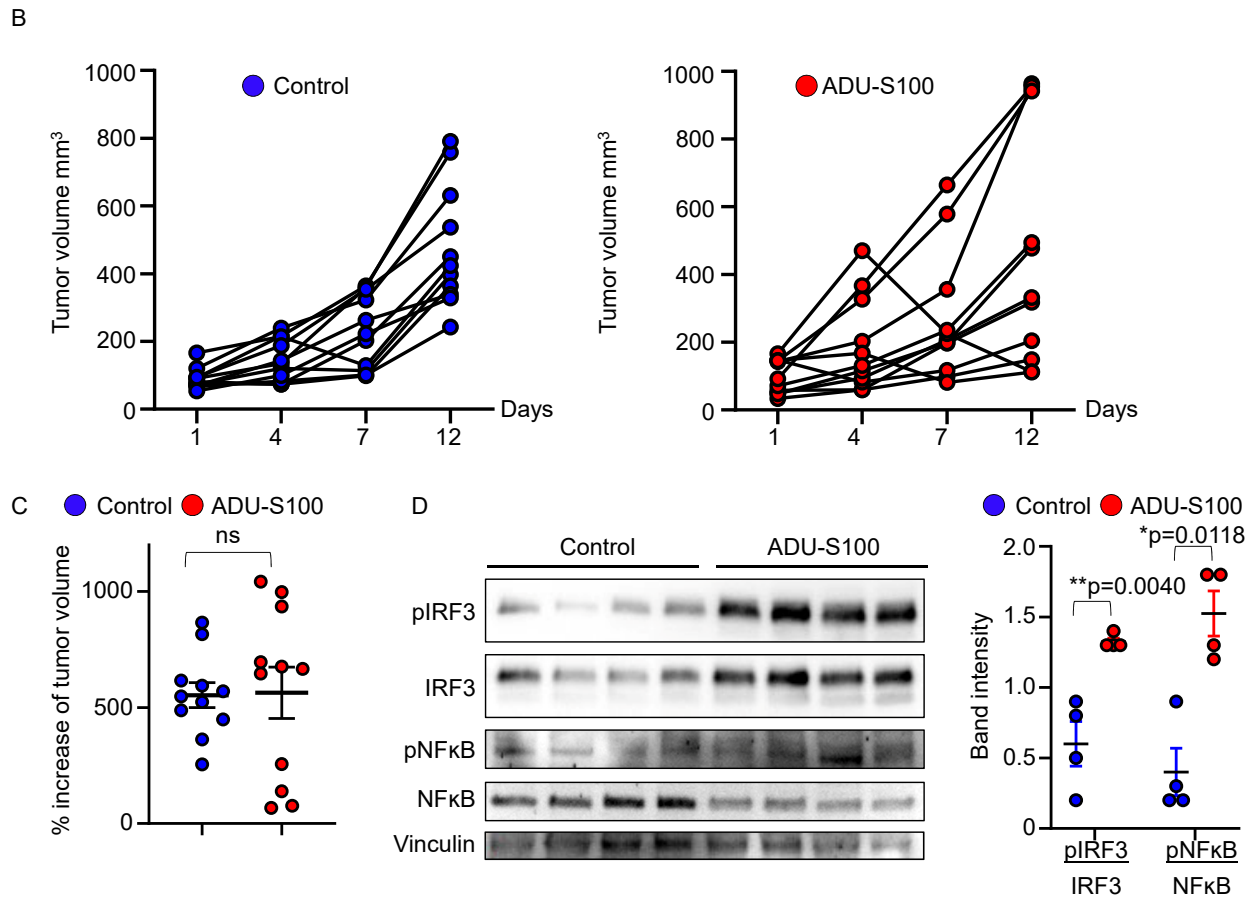
Supplemental Figure 1. STING agonist ADU-S100 activates the STING pathway in MPNST cell lines. (A) Western blot of the indicated cell lines and 2 cisMPNST tumors for PD-L1. The total PD-L1 band intensity normalized to that of vinculin is shown below each lane. (B) Western blot analysis for expression of the indicated proteins in mouse MPNST cell lines derived from *Nf1* and *p53* null skin progenitor cells (HTS-Luc MPNST) or harvested from *cisNP* mice (*cisMPNST*) treated with vehicle control (PBS) or ADU-S100. (C) Quantified protein band intensities from (B) are shown graphically. Data shown are as mean \pm SD. (D) PCR analysis of fold change in cytokine gene expression (*Ifnb1*, *Tnf*, *Cxcl10*, and *Il12a*) in MPNST cells as in (B) treated with PBS (n=3/ time point) or ADU-S100 (n=3/ time point). Data are represented as mean \pm SEM and p values are determined by Tukey's multiple comparisons test as indicated (D). ** $P < 0.01$.



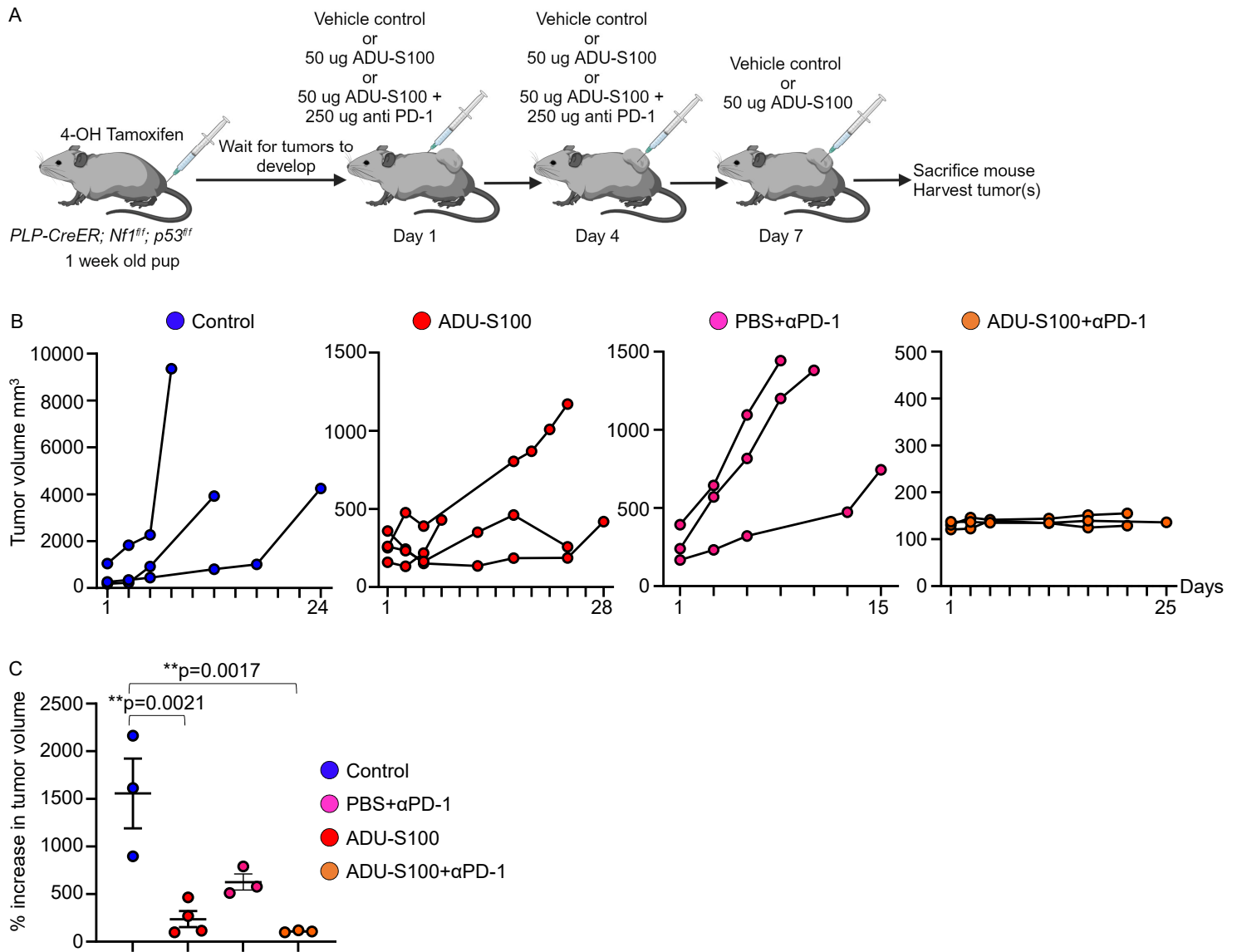
Supplemental Figure 2. SA3 treatment of *cisNP* mice activates the STING pathway in tumors. (A) Schema of SA3 treatment protocol. (B) Western blot analysis for expression of the indicated proteins in MPNSTs harvested from *cisNP* mice treated with vehicle control or SA3. Quantified protein band intensities for pIRF3/ IRF3 are shown graphically on the right. (C) PCR analysis of fold change in cytokine gene expression (*Ifnb1*, *Tnf*, *Cxcl10*, and *Il12a*) in *cis*MPNSTs harvested from control-treated (n=3) and SA3-treated (n=4) mice. (D) Paraffin sections of MPNSTs harvested from vehicle-treated or SA3 treated *cisNP* mice were stained with antibodies against CD3, CD4, CD8 α , PD-1, and PD-L1 and quantified (E). (F) Percent increase in tumor volume was measured in control-treated or SA3-treated *cisNP* mice. Data are represented as mean \pm SEM and p values are determined by two-tailed t test as indicated. * $P < 0.05$. Scale bar: 50 μ m.



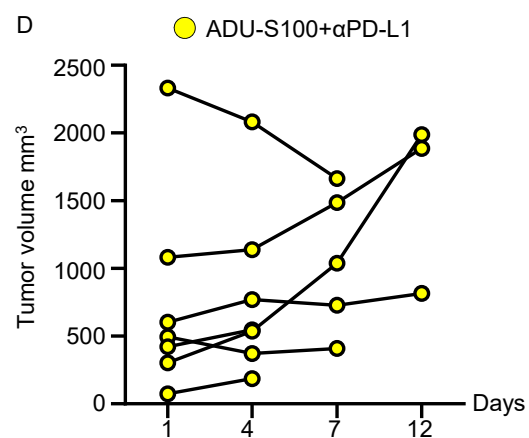
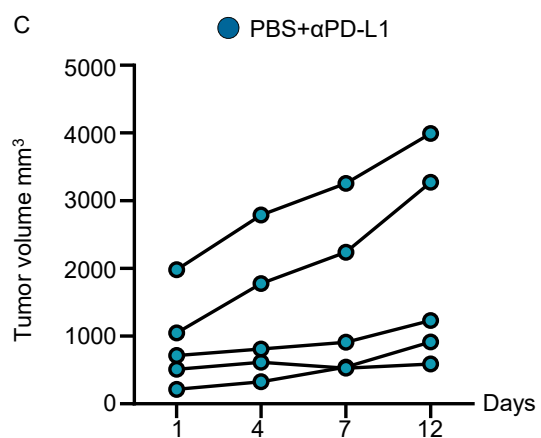
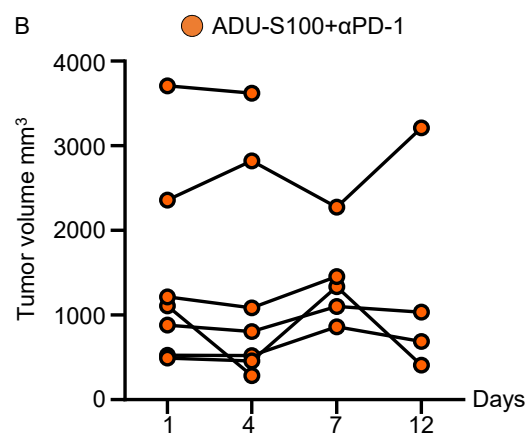
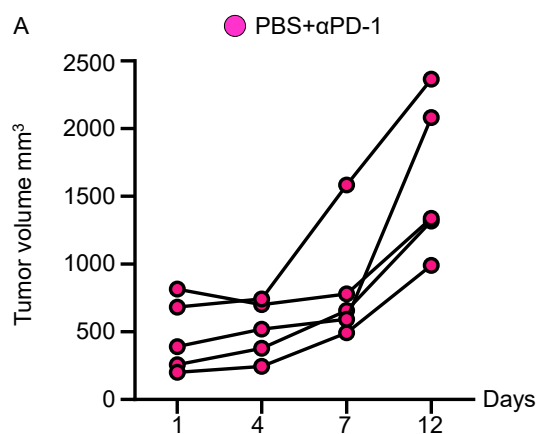
Supplemental Figure 3. *Foxp3* expression is unaltered upon ADU-S100 treatment. (A) Paraffin sections of murine spleen and control-treated (n=3) or ADU-S100-treated (n=3) *cis*MPNST are stained for FOXP3. Quantification of FOXP3-positive cells is shown on the right. (B) Western blot analysis for expression of FOXP3 in MPNSTs harvested from *cis*NP mice treated with vehicle control (n=7) or ADU-S100 (n=6). Quantified protein band intensities are shown graphically on the right. Data are represented as mean \pm SEM and p values are determined by unpaired t test as indicated. ns = not significant.



Supplemental Figure 4. STING agonist does not decrease MPNST volume in allograft MPNST in nude mice. (A) Schema of ADU-S100 treatment protocol in athymic nude mice bearing *cis*MPNST. (B) Tumor volume change over time in response to indicated treatments. (C) Tumor volume increase in athymic mice treated with PBS control (n=11) or ADU-S100 (n=11) as shown in (A). (D) Western blot analysis for expression of the indicated proteins in MPNSTs harvested from athymic mice treated with vehicle control (n=4) or ADU-S100 (n=4) for 24 hours. Quantified protein band intensities are shown graphically on the right. (E) PCR analysis of fold change in cytokine gene expression (*Ifnb1*, *Tnf*, *Cxcl10*, and *Il12a*) in *cis*MPNSTs harvested from control-treated (n=4) and ADU-S100-treated (n=4) athymic mice 24 hours after treatment. Data are represented as mean \pm SEM and p values are determined by two-tailed t test with respect to vehicle control. * $P < 0.05$, ** $P < 0.01$, ns = not significant.

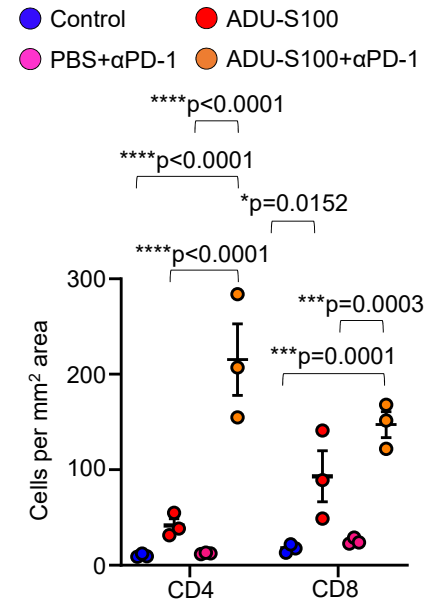
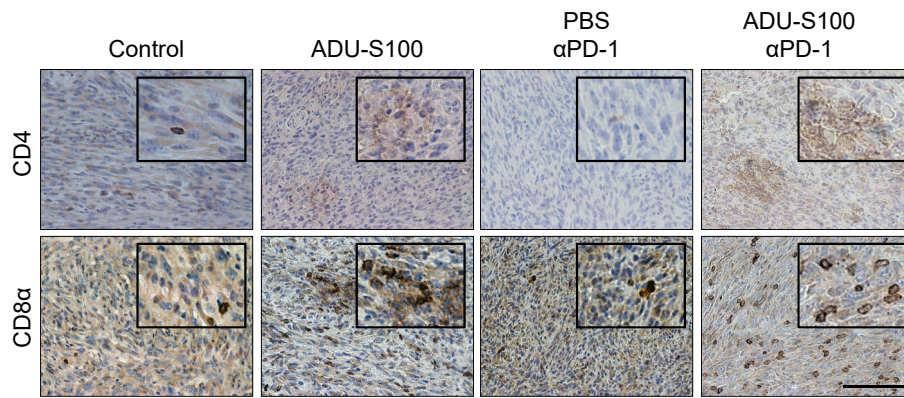


Supplemental Figure 5. Combination treatment of STING agonist and ICB decreases MPNST growth in *PLP-Cre; Nf1^{ff}; p53^{ff}* mice. (A) Schema of STING activation and ICB combination treatment protocol in *PLP-Cre; Nf1^{ff}; p53^{ff}* mice. (B) Tumor volume change of MPNST in *PLP-Cre; Nf1^{ff}; p53^{ff}* mice in response to the indicated treatments. (C) Percent increase in tumor volume in *PLP-Cre; Nf1^{ff}; p53^{ff}* mice upon indicated treatments. Control, n=3; ADU-S100, n=4; PBS + α PD-1, n=3; ADU-S100 + α PD-1, n=3. Data are represented as mean \pm SEM and p values are determined by Tukey's multiple comparisons test as indicated. * $P < 0.05$, ** $P < 0.01$.

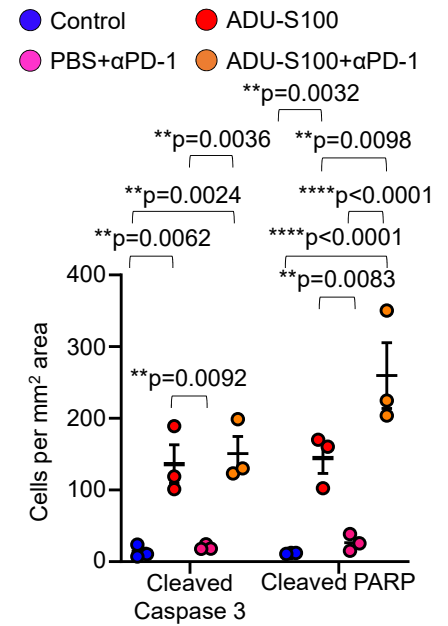
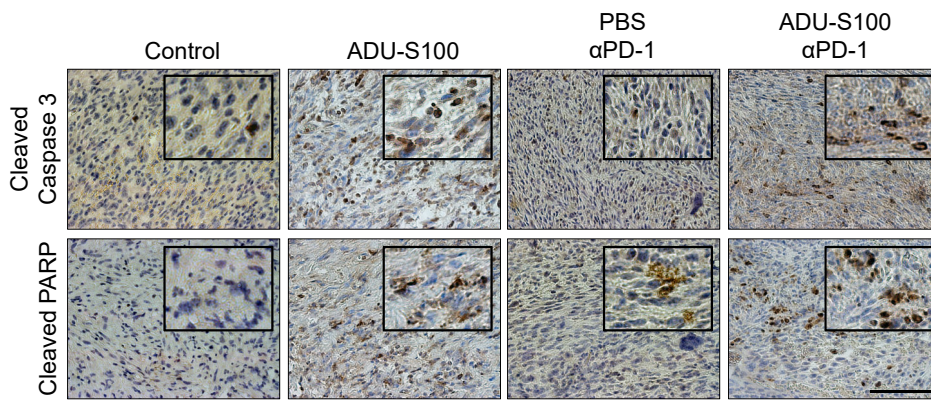


Supplemental Figure 6. Combination treatment of *cis*MPNSTs with STING activation plus ICB slows tumor growth. Tumor volume change over time in *cisNP* mice treated with (A) PBS + α PD-1, (B) ADU-S100 + α PD-1, (C) PBS + α PD-L1, or (D) ADU-S100 + α PD-L1.

A

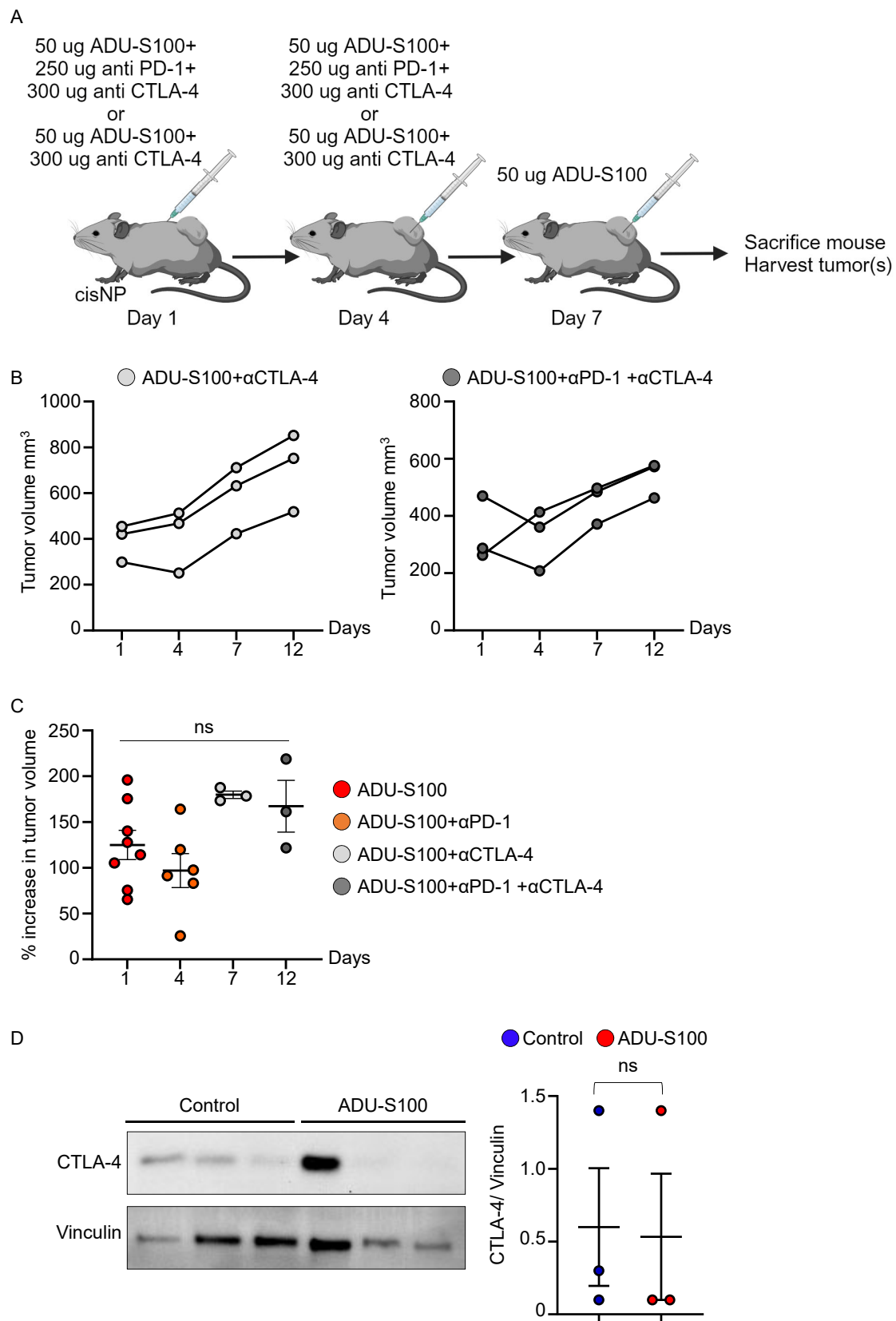


B



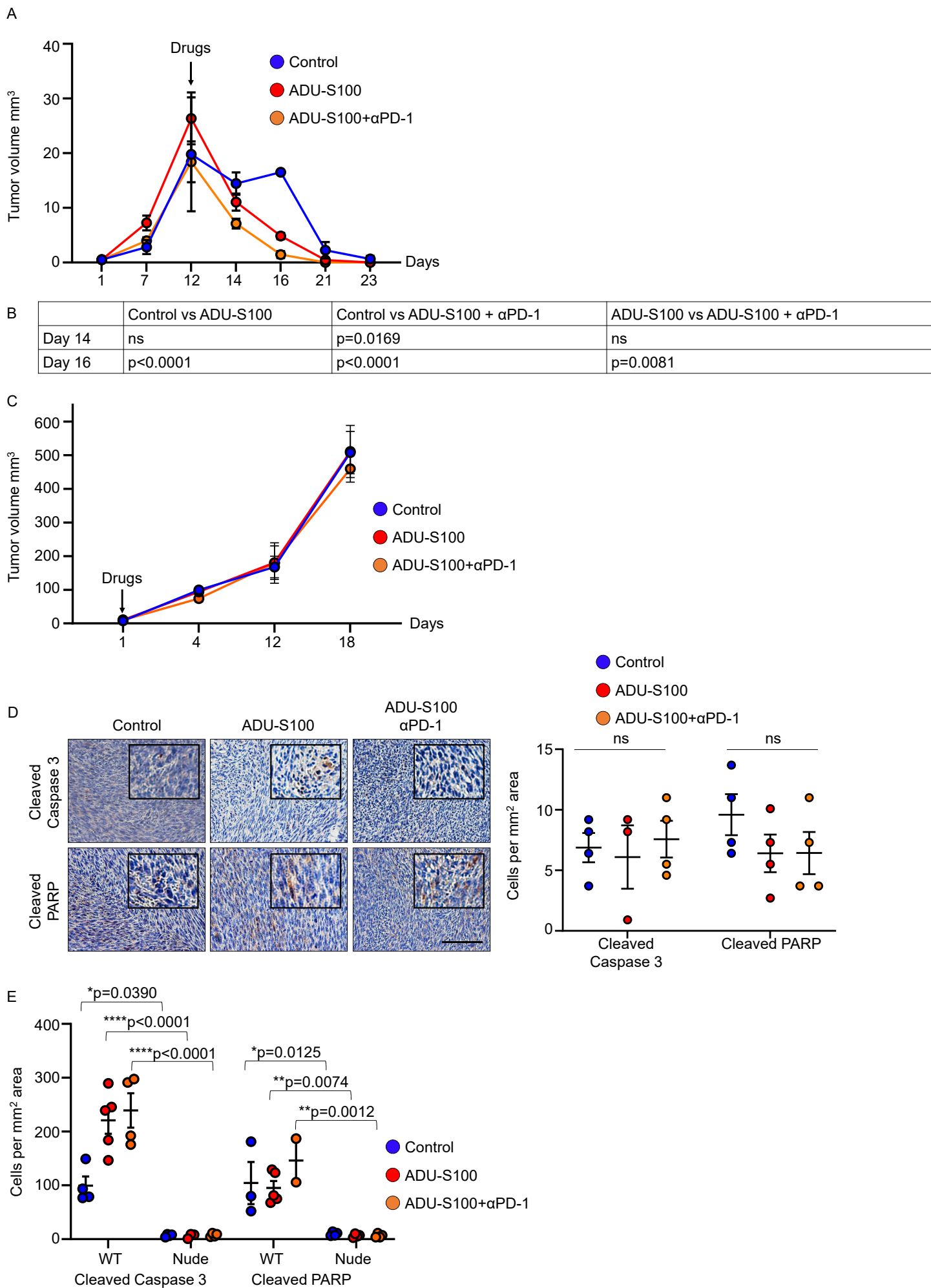
Supplemental Figure 7. Combination treatment of STING agonist plus ICB increases T cell infiltration and expression of apoptotic markers in MPNST in *PLP-Cre; Nf1^{ff}; p53^{ff}* mice.

(A) Paraffin sections from MPNSTs harvested from *PLP-Cre; Nf1^{ff}; p53^{ff}* mice treated as indicated were stained for T cell markers. Quantification of images are shown on the right. (B) Paraffin sections from MPNSTs in (A) stained for Cleaved Caspase 3 and Cleaved PARP. Quantification of images are shown on the right. Control, n=3; ADU-S100, n=3; PBS + α PD-1, n=3; ADU-S100 + α PD-1, n=3. Data are represented as mean \pm SEM and p values are determined by Tukey's multiple comparisons test as indicated. * $P < 0.05$, ** $P < 0.01$, *** $P < 0.001$. Scale bar: 50 μ m.



Supplemental Figure 8. Combination treatment of STING agonist plus α PD-1 and α CTLA-4 antibodies does not further decrease MPNST volume compared to STING agonist plus α PD-1 treatment.

(A) Schema of ADU-S100 plus α PD-1 and α CTLA-4 treatment protocol in *cisNP* mice. (B) Tumor volume changes in response to the indicated treatments. (C) Percentage increase in tumor volume upon indicated treatments. Data sets for ADU-S100 and ADU-S100 plus α PD-1 used in this graph are borrowed from Figure 4D for clarity and ease of comparison. ADU-S100 + α CTLA-4, n=3; ADU-S100 + α PD-1 + α CTLA-4, n=3. (D) Western blot analysis for expression of CTLA-4 in MPNSTs harvested from *cisNP* mice treated with vehicle control (n=3) or ADU-S100 (n=3). Quantified protein band intensities are shown graphically on the right. Data are represented as mean \pm SEM and p values are determined by Tukey's multiple comparisons test in (C) and two-tailed t test in (D) as indicated. ns = not significant.



Supplemental Figure 9. Combination treatment of STING activation plus ICB accelerates tumor regression in a human MPNST xenograft mouse model. (A) Difference in tumor volume in human MPNST xenograft mice upon treatment with PBS (n=15), ADU-S100 (n=15), or ADU-S100 + α PD-1 (n=15). (B) Statistical significance of the volume differences in (A) determined by multiple unpaired t tests. (C) Difference in tumor volume in human MPNST xenograft in nude mice upon treatment with PBS (n=4), ADU-S100 (n=4) or ADU-S100 + α PD-1 (n=4). (D) Paraffin sections from nude mouse xenograft MPNST treated as indicated were stained for Cleaved Caspase 3 and Cleaved PARP. (E) Comparison of Cleaved Caspase 3 and Cleaved PARP levels in wild-type mouse (repeated from data in Figure 6D) and nude mouse xenograft MPNST. Data are represented as mean \pm SEM and p values are determined by Tukey's multiple comparisons test as indicated. Scale bar: 50 μ m. * P < 0.05, ** P < 0.01, *** P < 0.001, ns = not significant.

Supplemental Table 1: Primer sequences for qRT-PCR

<i>Ifnb1</i>	mIfnb1-F1	5' CCC TAT GGA GAT GAC GGA GA 3'
	mIfnb1-R1	5' ACC CAG TGC TGG AGA AAT TG 3'
<i>Tnf</i>	mTnf-F1	5' ACG GCA TGG ATC TCA AAG AC 3'
	mTnf-R1	5' GTG GGT GAG GAG CAC GTA GT 3'
<i>Cxcl10</i>	mCxcl10-F1	5' GCT GCA ACT GCA TCC ATA TC 3'
	mCxcl10-R1	5' GTG GCA ATG ATC TCA ACA CG 3'
<i>Il12a</i>	mIl12a-F1	5' CTC CTG TGG GAG AAG CAG AC 3'
	mIl12a-R1	5' CAG ATA GCC CAT CAC CCT GT 3'